BioMedical Engineering OnLine

RESEARCH Open Access

Predictors of flatfoot in 11–12-year olds: a longitudinal cohort study

Tomoko Yamashita[1,2*], Mitsuru Sato[3], Shingo Ata[2] and Kazuhiko Yamashita[1,4]

*Correspondence:
tomoko.yamashita@tohto.ac.jp

[1] Department of Clinical Engineering, Faculty of Human Care at Makuhari, Tohto University, 1-1 Hibino, Mihama-Ku, Chiba 261-0021, Japan
[2] Department of core informatics, Graduate School of Informatics, Osaka Metropolitan University, Osaka, Japan
[3] Department of Physical Therapy, Faculty of Rehabilitation, Gunma Paz University, Gunma, Japan
[4] Department of Information Systems, Graduate School of Engineering, Saitama Institute of Technology, Saitama, Japan

Abstract

Background: The structures around the navicular bones, which constitute the medial longitudinal arch, develop by 10 years of age. While navicular bone height is often emphasized in the assessment of flatfoot, three-dimensional (3D) evaluations, including those of structural parameters during inversion, have rarely been investigated. If the development of flatfoot during the growth process could be predicted, appropriate interventions could be implemented. Therefore, in this longitudinal cohort study, we developed a system, utilizing smartphones, to measure the 3D structure of the foot, performed a longitudinal analysis of changes in midfoot structures in 124 children aged 9–12 years, and identified factors influencing the height of the navicular bone. The foot skeletal structure was measured using a 3D system.

Results: Over 2 years, foot length and instep height increased during development, while navicular height decreased. The 25th percentile of the instep height ratio and navicular height ratio at ages 9–10 years did not exceed those at ages 11–12 years, with percentages of 17.9% and 71.6%, respectively, for boys, and 15.8% and 49.1%, respectively, for girls. As the quartiles of the second toe–heel–navicular angle (SHN angle) increased at ages 9–10 years, the axis of the bone distance (ABD) and SHN angles at ages 11–12 years also increased, resulting in a decrease in the navicular height ratio. A significant inverse correlation was found between changes in SHN angle and navicular height ratio. These findings indicate that the navicular bone rotation of the midfoot is a predictor of the descent of the navicular bone.

Conclusions: This study revealed that some children exhibit decreases in navicular bone height with growth. As a distinct feature, the inversion of the navicular bone promotes flattening of the midfoot. Thus, this study provides insights into changes in midfoot development in children and provides an effective evaluation index.

Keywords: CT-based 3D analysis, Foot 3D scanner, Medial longitudinal arches, Elementary school student

Background

The foot is composed of three intersecting arches—the medial longitudinal arch, lateral longitudinal arch, and transverse arch—all located at the height of the distal tarsal bones, and they develop during the first 10 years of life [1, 2]. The medial longitudinal arch, which is composed of the calcaneus; talus; navicular; cuneiform; and first, second, and

third metatarsal bones, is a particularly important structure with a high degree of height and flexibility, allowing for dynamic changes in shape and structure while walking [3].

The height of the medial longitudinal arch is determined by the characteristics of the subtalar joint complex, while its shape under static load is determined by the interaction between the shape of the muscles and bones and the strength and flexibility of the ligaments [4]. The size of the foot, strength of the ligaments and muscles, and relevant motor ability all develop during the growth and maturation periods [5]. The factors necessary for successful arch development include appropriate ossification and alignment, particularly at the sustentaculum tali and navicular bone, as well as healthy soft tissue stabilizers [6].

The flatfoot deformity is characterized by a drop in the medial longitudinal arch, eversion of the hindfoot, and abduction of the forefoot under loading [3]. The incidence of flatfoot is known to decrease with age; however, the precise incidence at each age remains poorly understood [7].

Previous studies evaluating flatfoot have examined footprints, photographs, and height of the navicular bone [8–11]. A footprint reflects the ground contact status; however, this is insufficient for skeletal evaluation [12]. Assessment of the medial longitudinal arch, which is formed by the height of the navicular bone, is useful in two-dimensional analyses. However, the anatomical movement of the navicular bone is an inversion caused by loading, defined as a three-dimensional (3D) motion. Detailed anatomical analyses of the complex tarsal bones in addition to 3D structural analyses are needed for anatomical analysis of flatfoot [13, 14]. Computed tomography (CT)-based 3D analysis requires the application of a load to the sole of the foot in the supine position [15]. However, this method does not adequately reflect standing posture and cannot be applied to healthy children because of the exposure to X-rays.

In previous studies, flatfoot was considered to be predominantly caused by the relaxation of the spring ligament, which includes the three bones of the calcaneus–subtalar joint complex and the calcaneonavicular ligament [16]. The spring ligament develops during a certain period in children and is influenced by movement-related stimuli. However, longitudinal studies of the 3D changes in the midfoot of the same child are lacking.

Furthermore, the impact of insufficient physical activity on foot development in healthy children is not yet clear. In particular, activity restrictions owing to the widespread outbreak of coronavirus disease (COVID-19) may have affected foot development in children. Actively imposing activity restrictions on children to study foot growth is not feasible from an ethical perspective; however, measuring foot development during periods of restricted activity as an environmental factor could be informative. In addition, there is still a lack of non-invasive, simple, quantitative methods for measuring the foot.

To address this knowledge gap, in the present study, we developed a system to measure the shape of the foot surface without using X-rays [17, 18]. We aimed to use this system to longitudinally measure the characteristics of the feet of elementary school students in the developmental stage of the musculoskeletal system and to identify factors influencing changes in the shape of the midfoot, particularly the height of the navicular bone. Furthermore, we clarified the usefulness of the foot skeleton evaluation indices developed in this study.

Table 1 Changes in the measurement results over 2 years

		9–10 years old	11–12 years old	*p*-value
Foot length [cm]	Male	20.71 ± 1.13	22.72 ± 1.33	< 0.001
	Female	20.39 ± 1.19	21.97 ± 1.04	< 0.001
IH [cm]	Male	5.58 ± 0.46	6.24 ± 0.56	< 0.001
	Female	5.39 ± 0.48	5.93 ± 0.5	< 0.001
NH [cm]	Male	3.46 ± 0.49	3.21 ± 0.64	< 0.001
	Female	3.13 ± 0.53	2.99 ± 0.54	0.095
IH rate [%]	Male	26.99 ± 1.9	27.51 ± 2.2	0.016
	Female	26.47 ± 2.01	27.04 ± 2.16	0.03
NH rate [%]	Male	16.78 ± 2.37	14.1 ± 2.74	< 0.001
	Female	15.3 ± 2.48	13.65 ± 2.61	< 0.001
SHN angle [degrees]	Male	24.83 ± 2.89	22.44 ± 2.81	< 0.001
	Female	25.11 ± 2.67	23.37 ± 2.39	< 0.001
ABD [cm]	Male	0.94 ± 0.5	0.89 ± 0.45	0.355
	Female	1.15 ± 0.46	1.02 ± 0.43	0.027
ABD rate [%]	Male	4.55 ± 2.40	3.93 ± 1.93	0.015
	Female	5.60 ± 2.24	4.67 ± 1.98	< 0.001

IH, instep height; NH, navicular height; SHN, second toe–heel–navicular; ABD, axis of the bone distance

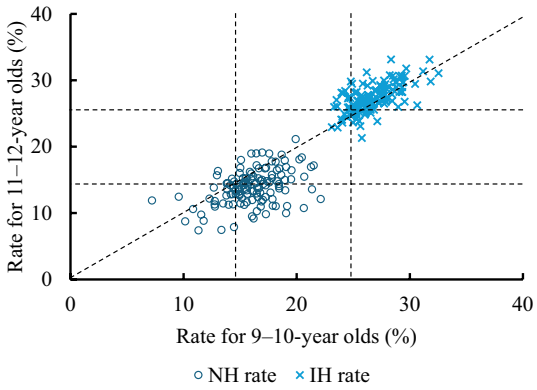

Fig. 1 Scatter plots of NH and IH for 9–10- and 11–12-year-old participants

Results

Changes in measurement results over the 2-year period

As shown in Table 1, the FL, IH, and IH rates increased significantly over the 2-year study period. In contrast, the NH and NH rate decreased significantly, although the former trend was only significant in boys. Both the SHN angle and ABD rate decreased, and the position of the navicular bone shifted in a direction that reduced the discrepancy in the skeletal structure.

Scatter plots were used to visualize the measurement data obtained at 9 and 10 years of age for the NH and IH rates on the horizontal axis and at 11 and 12 years of age on the vertical axis. In Fig. 1, values positioned below the diagonal line indicate a decline from ages 9–10 years to 11–12 years. In many cases, the NH rate was below the diagonal line. The proportions of children who did not exceed the 25th percentile values for the IH and NH rates at 11 and 12 years of age, which was achieved at 9 and 10 years of age, were as

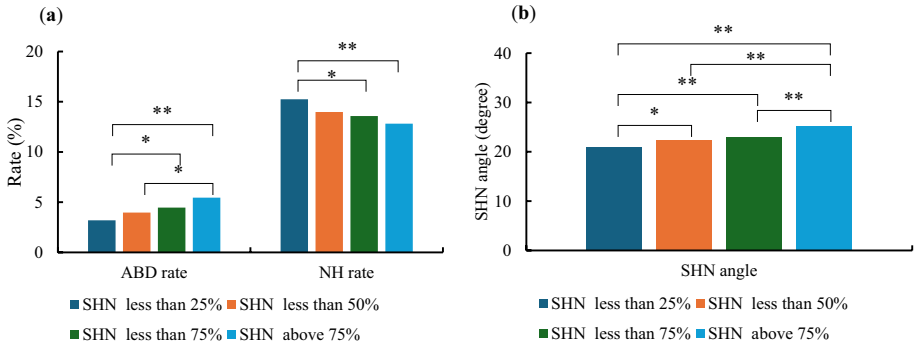

Fig. 2 Foot skeletal structure according to the quartiles of the SHN angle for the 9–10-year olds. **a** ABD rate and NH rate, **b** the SHN angle for the 11–12-year-old participants, classified by the quartiles of the SHN angle for the 9–10-year-old participants. *$p < 0.05$; **$p < 0.01$. ABD, axis of the bone distance; NH, navicular height; SHN, second toe–heel–navicular angle

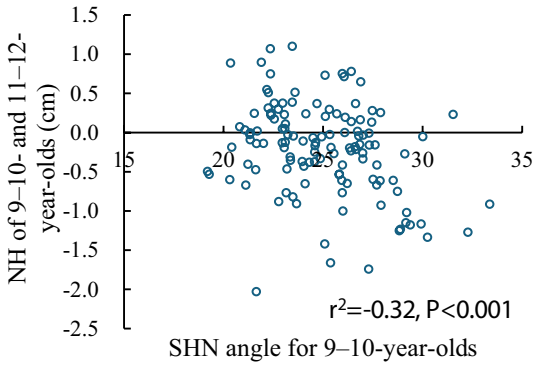

Fig. 3 Scatter plot of SHN angle and differences between NH of 9–10- and 11–12-year olds. NH, navicular height; SHN, second toe–heel–navicular angle

follows: the IH rate was 17.9% in boys and 15.8% in girls, and the NH rate was 71.6% in boys and 49.1% in girls.

Dotted lines are drawn on the horizontal axis and vertical axis at the first quartile of the NH and IH rates at the age of 9–10 years. Data points above the diagonal dotted line indicate an improvement in values. The first quartile values are as follows: NH rate, 14.6%; IH rate, 25.2%; IH, instep height; NH, navicular height; SHN, second toe–heel–navicular.

Changes in skeletal structure and NH rate at 11–12 years of age based on the quartile of the SHN angle at 9–10 years of age

Figure 2 shows the ABD rate, NH rate, and SHN angle in participants at 11–12 years of age based on the quartiles of the SHN angle at 9–10 years of age. As the SHN angle at 9–10 years of age increased, the ABD and SHN angles at 11–12 years of age also increased significantly and the NH rate decreased significantly.

Figure 3 shows the changes in NH height at 9–10 and 11–12 years of age based on the SHN angle at 9–10 years of age on the horizontal axis. The vertical axis represents an increase in NH with a positive sign and a decrease with a negative sign. There was a significant correlation between the changes in the SHN angle and NH rate ($r = -0.32$,

Table 2 Results of the multiple regression analysis of the SHN angle in 11–12-year-old participants

Variable	B	SE B	B	*p*-value	r^2	Adjusted r^2
SHN angle for 9–10-year olds	0.54	0.07	0.56	< 0.001	0.39	0.38
IH rate for 9–10-year olds	− 0.22	0.10	− 0.16	0.03	F-value	*p*-value
					38.51	< 0.001

Dependent variable: SHN angle for 11–12-year-old participants

SHN, second toe–heel–navicular; IH, instep height

Table 3 Results of the multiple regression analysis of the NH rate in 11–12-year-old participants

Variable	B	SE B	β	*p*-value	r^2	Adjusted r^2
IH rate for 9–10-year olds	0.56	0.10	0.41	< 0.001	0.46	0.44
ABD rate for 9–10-year olds	− 0.20	0.09	− 0.18	0.03		
NH rate for 9–10-year olds	0.30	0.08	0.28	< 0.001	*F*-value	*p*-value
SHN angle for 9–10-year olds	− 0.16	0.07	− 0.17	0.03	25.32	< 0.001

Dependent variable: NH rate for 11–12-year-old participants

IH, instep height; ABD, axis of the bone distance; NH, navicular height; SHN, second toe–heel–navicular

$p < 0.001$). These results show that when the SHN angle at 9–10 years of age was large, the proportion of those with a decreased NH rate 2 years later was higher.

Multiple regression analysis to predict the SHN angle and NH rate at 11–12 years of age

A multiple regression analysis was performed using a stepwise method to predict the SHN angle and NH rate at 11–12 years of age, with the SHN angle, IH rate, NH rate, and ABD rate as the independent variables at 9–10 years of age and the SHN angle and NH rate as the dependent variables at 11–12 years of age.

As shown in Table 2, the predictors for the SHN angle at 11–12 years of age were the SHN angle and IH rate at 9–10 years of age, with β values of 0.56 and − 0.16, respectively, and an adjusted R^2 of 0.39, indicating moderate prediction accuracy. As shown in Table 3, the predictors for the NH rate at 11–12 years of age were the IH rate, ABD rate, NH rate, and SHN angle at 9–10 years of age, with β values of 0.41, − 0.18, 0.28, and − 0.17, respectively, and an adjusted R^2 of 0.46.

Discussion

Herein, we describe the results of a 2-year longitudinal study investigating the development of the midfoot in elementary school children. In particular, we conducted 3D measurements of the surface structure of the foot, focusing on the height of the navicular bone, a known indicator of flatfoot, in addition to the lateral displacement and misalignment of the foot skeleton. Features of the feet were extracted to predict the navicular bone height 2 years later.

Our analysis clearly showed that the FL and IH increased, while the SHN angle and ABD rate decreased from the overall mean, indicating strong development over the 2 years of follow-up. However, the NH rate, which constitutes the midfoot, decreased. Reportedly, the medial longitudinal arch develops around 10 years of age [1, 2], while the FL increases in boys and girls until 15 and 13 years of age, respectively [19]. In the present study, FL increased, while NH showed a lower rate of increase than FL or a decrease.

As shown in Fig. 1, the thickness of the foot is still increasing at 12 years of age as the IH increased significantly, while the NH rate decreased significantly over the 2-year period. In previous studies, NH increased significantly from 6 to 13 years of age; at 9 years of age, it was 2.89 cm for boys and 2.79 cm for girls, increasing to 3.48 cm and 3.39 cm, respectively, at 12 years of age [20]. In the present study, the NH decreased significantly from 3.46 cm for boys and 3.13 cm for girls at 9 and 10 years of age, respectively, to 3.21 cm and 2.99 cm at 11 and 12 years of age, respectively. The NH at the bottom quartile of the SHN angle at 9 and 10 years of age was 3.63 cm for boys and 3.14 cm for girls, while the NH at the lower quartile was 3.30 cm and 3.15 cm, the NH at the upper quartile was 3.14 cm and 2.87 cm, and the NH at the top quartile was 2.79 cm and 2.79 cm, respectively. In the present study, the NH increased slightly or remained the same as that in the 9–10-year-old participants. These values were almost equivalent to those found in previous studies. Although there was a difference in study design (i.e., a longitudinal study vs. the previous cross-sectional design), it is presumed that particular factors influenced the development. During the study period, which coincided with the COVID-19 pandemic, elementary school students' outings were restricted, and their physical education classes were limited. As extracurricular sports were also not conducted, the reduction in physical activity might have had an impact on their foot measurements.

Generally, the development of children's feet progresses in terms of both size and height. Even with the exercise restrictions imposed owing to COVID-19, which limited stimuli necessary for muscle and ligament development, the development of the feet could not be halted, potentially leading to deformities. Therefore, we speculate that the axis of midfoot development shifted inward, inducing pronation.

From these results, as shown in Fig. 2, when the SHN angle was large, i.e., when the navicular bone (point e in Fig. 4) was far from the centerline a–b, the ABD and SHN angles became larger, and the NH rate decreased after 2 years. In other words, it was not

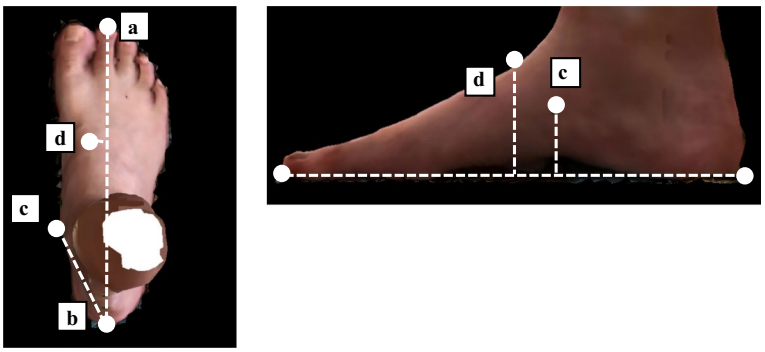

Fig. 4 Outputs of the three-dimensional (3D) foot scanning system. The positions of the second toe tip (**a**), heel (midpoint of the width of the calcaneal tuberosity) (**b**), navicular bone (**c**), and instep (**d**) were identified as feature points using the 3D foot scanner. In the present study, five 3D foot skeletal indices were used, including the distance from the heel to the tip of the second toe (foot length [FL: Line a–b]), height of the navicular bone from the floor (navicular height [NH: Line c]), distance from the floor to the highest point of the talus head (instep height [IH: Line d]), second toe–heel–navicular angle (SHN angle: angle made by abc), and the distance from the center line (Line a–b) when the coordinate point of the talus head is projected onto the floor (axis of the bone distance [ABD: Line ab-d]). The derived distance information is influenced by the FL; therefore, normalization was performed with the distance from the heel to the tip of the second toe as a reference (e.g., NH/FL = NH rate)

the increase in FL that decreased the NH ratio but rather the increase in the SHN angle, indicating an NH inversion, resulting in insufficient vertical growth of NH.

In addition, as shown in Fig. 3, when the SHN angle is larger at ages 9–10 years, the NH is lower at ages 11–12 years than it was at ages 9–10 years. Previous studies have not investigated the lateral displacement of the navicular bone; however, this study yielded different results in terms of changes in NH [20]. The anatomical reasons for this increase in the SHN angle are believed to include the relaxation of the spring ligament, which includes the calcaneonavicular joint complex, known to be a factor in flatfoot [14]. An increase in the SHN angle indicates an increase in the inversion of the navicular bone.

The navicular bone is connected to the medial and intermediate cuneiform bones, and instability may occur between the first and second metatarsal bones, potentially resulting in greater mobility between the two metatarsal bones [21]. Therefore, flattening of the midfoot may lead to sports injuries, hallux valgus, deformities of the heel bone, pes planus, and other basic musculoskeletal characteristics that could lead to decreased future walking function [3, 22, 23]. The SHN angle from this system is a useful indicator of internal rotation of the navicular bone.

Factors predicting SHN and NH rates were derived from the SHN angle, IH, NH, and ABD 2 years prior. Lateral displacement of the navicular bone, foot thickness, and foot distortion are also related.

As demonstrated above, evaluation indices that assess pronation should be used rather than focusing solely on the height of the navicular bone in relation to flat feet. This is because both the navicular and medial cuneiform bones are involved in the development of the midfoot in children. In other words, this study has revealed that the changes in the midfoot of children can be evaluated using the newly developed 3D measurement indices: the SHN angle, ABD, NH, and IH.

Limitations

The foot 3D scanner developed in the present study measures the surface structure of the foot; therefore, it does not consider the fat layer of the foot, which may influence the measurement results to some degree. The study period included the COVID-19 pandemic, and there may be variability in physical activity. However, we expect our findings to adequately reflect the impact of the suppression of physical activity on NH, providing a predictive factor for growth 2 years later.

Conclusions

This study clarified the changes in midfoot development in children and demonstrated the usefulness of the evaluation indicators identified in this study. The development of the musculoskeletal and ligament functions that constitute the midfoot structure is important in the development of the midfoot structure in children. An increase in the SHN angle represents a state of internal rotation of the navicular bone, which may trigger an increase in ABD. The midfoot plays an important role in shock absorption during the up-and-down movement of the navicular bone. An increase in the SHN angle, decrease in the NH rate, or increase in the ABD may all indicate a decrease in the function, or incomplete development of the muscles and ligaments, of the midfoot. This may lead to an increase in joint diseases, such as knee osteoarthritis, in the future.

Methods

Participants

This study was conducted between July 2019 and July 2022. The participants included 124 individuals (67 male and 57 female) aged 9–10 years from 2019 to 2020 and 11–12 years from 2021 to 2022. Participants were recruited from an elementary school; all students within the age range and whose parents provided consent were initially enrolled. The following participants were excluded: individuals who could not participate in the measurements or who had orthopedic problems such as foot fractures.

All participants experienced a period of reduced physical activity and outings due to the COVID-19 pandemic from 10 to 12 years of age. The self-restraint period during the COVID-19 pandemic was as follows. The Japanese Ministry of Health, Labour and Welfare issued a directive on February 20, 2020, for self-imposed restrictions on going out to reduce the likelihood of infection. This was followed by an announcement of the rapid spread of COVID-19 on March 10, 2020, and the declaration of a state of emergency on April 8, 2020. The state of emergency was lifted on May 25, 2020, and on May 22, 2022, the Ministry of Education, Culture, Sports, Science and Technology announced that there was no longer an obligation to wear masks indoors and outdoors at schools. As the skeletal structure of the midfoot develops until 10 years of age [1, 2], the development of muscle strength and ligaments would presumably be affected in this participant group.

This study was approved by the Ethics Review Committee of Tohto University (Approval Number: R0306) and was conducted in accordance with the tenets of the Declaration of Helsinki. Consent was obtained from the elementary school where the experiment was conducted and from the parents of the students who were included in the study.

Measurement methods

Our newly developed 3D measurement system was used to assess the skeletal structure of the foot. The foot feature points were identified by a physical therapist. Figure 4 shows the 3D reconstruction outputs of this system. The measurements were conducted using commercially available smartphones, capturing the area around the participant's foot. Care was taken to ensure that the foot remained within the frame, although minor shaking would not affect the analysis. The image-capturing process took approximately 10 s. Video files were stored on a server, and the developed program was used to 3D-reconstruct the foot and identify feature points. The spatial resolution of the system was 1.7 mm for distance and 0.1 degree for angle [17, 18]. The accuracy of the developed 3D foot scanner is shown in the Appendix of a previous study [17].

During the measurements, the standing foot width was 22 cm for the toes and 18 cm for the heels. To 3D-reconstruct the foot's skeletal structure, the inner side of the foot must also be captured, requiring a certain foot width to be set. Therefore, we experimentally determined the optimal foot width for 3D reconstruction of the foot's skeletal structure. All participants underwent measurements at school when they were aged between 9 and 10 years and again when they were aged between 11 and 12 years.

Statistical analysis

SPSS (version 28; IBM SPSS Statistics, Armonk, NY, USA) was used to analyze the data. The results are presented as means and standard deviations. The Shapiro–Wilk test was performed to assess the distribution of the data, and the data were considered normally distributed at p values ≥ 0.05.

Paired t-tests were used to compare the measured values with the corresponding reference data. One-way analysis of variance with Tukey's post hoc test was used to analyze the measurement values of each quartile of the NH rate and the SHN angle. Relationships between variables were explored by calculating Pearson's correlation coefficients. A multiple linear regression analysis was performed to predict the SHN angle and NH rate for 11- and 12-year-old participants based on the 3D scanner measurement results. Statistical significance was set at p values < 0.05.

The sample size was determined to be 57, assuming an effect size of 0.5, significance level of 0.05, and power of 0.95 for the expected outcome of the NH. Assuming a dropout rate of 30% at the 2-year follow-up, 74 participants were required.

Based on the measurement results, we calculated the detection power for FL, NH, IH, and the SHN angle at ages 9–10 years and 11–12 years. The results showed that the detection power for FL was 1.0, that for NH was 0.94, that for IH was 1.0, and that for the SHN angle was 0.80, confirming sufficient detection power.

Abbreviations

3D	Three-dimensional
ABD	Axis of the bone distance
COVID-19	Coronavirus disease 2019
CT	Computed tomography
FL	Foot length
IH	Instep height
M1	First metatarsal bone
M2	Second metatarsal bone
NH	Navicular height
SHN	Second toe–heel–navicular angle

Acknowledgements

Not applicable.

Author contributions

TY and KY planned the study, supervised the data analysis, and wrote the paper. TY, MS, SA and KY performed all measurements and contributed to data acquisition. TY, MS, SA and KY performed all statistical analyses and contributed to revising the paper. All the authors read and approved the final manuscript.

Funding

This work was supported by JSPS KAKENHI [grant numbers 23K19225, 22H03995], CASIO Science Promotion Foundation, and Telecommunications Advancement Foundation. The funders had no involvement in the study design; data collection, analysis, or interpretation; writing of the report; or decision to submit the article for publication.

Availability of data and materials

The datasets used or analyzed in the current study are available from the corresponding author on reasonable request.

Declarations

Ethics approval and consent to participate

This study was approved by the Ethics Review Committee of Tohto University (Approval Number: R0306). The study was conducted in accordance with the tenets of the Declaration of Helsinki. As participants were recruited from an elementary school, their parents provided consent for participation in this study.

Consent for publication

Consent for publication was obtained from the elementary school where the experiment was conducted as well as from the parents of the students who were included in the study.

Competing interests
The authors declare that they have no competing interests.

Received: 17 March 2024 Accepted: 9 August 2024
Published online: 21 August 2024

References

1. Cappello T, Song KM. Determining treatment of flatfeet in children. Curr Opin Pediatr. 1998;10:77–81.
2. Rodriguez N, Volpe RG. Clinical diagnosis and assessment of the pediatric pes planovalgus deformity. Clin Podiatr Med Surg. 2010;27:43–58.
3. Van Boerum DH, Sangeorzan BJ. Biomechanics and pathophysiology of flatfoot. Foot Ankle Clin. 2003;8:419–30.
4. Hicks JH. The mechanics of the foot I. Joints J Anat. 1953;87:345–57.
5. Bosch K, Gerss J, Rosenbaum D. Development of healthy children's feet—nine-year results of a longitudinal investigation of plantar loading patterns. Gait Posture. 2010;32:564–71.
6. Gould N, Moreland M, Alvarez R, Trevino S, Fenwick J. Development of the child's arch. Foot Ankle. 1989;9:241–5.
7. Uden H, Scharfbillig R, Causby R. The typically developing paediatric foot: how flat should it be? A systematic review. J Foot Ankle Res. 2017;10:37.
8. Gilmour JC, Burns Y. The measurement of the medial longitudinal arch in children. Foot Ankle Int. 2001;22:493–8.
9. Aenumulapalli A, Kulkarni MM, Gandotra AR. Prevalence of flexible flat foot in adults: a cross-sectional study. J Clin Diagn Res. 2017;11:AC17-20.
10. Elvan A, Simsek IE, Cakiroglu MA, Angin S. Association of quadriceps angle with plantar pressure distribution, navicular height and calcaneo-tibial angle. Acta Orthop Traumatol Turc. 2019;53:145–9.
11. Mall NA, Hardaker WM, Nunley JA, Queen RM. The reliability and reproducibility of foot type measurements using a mirrored foot photo box and digital photography compared to caliper measurements. J Biomech. 2007;40:1171–6.
12. Yamashita T, Yamashita K, Sato M, Ata S. Differences in foot features between children and older adults assessed using a three-dimensional foot scanning system: a cross-sectional observational study. Adv Biomed Eng. 2022;11:172–8.
13. Imai K, Tokunaga D, Takatori R, Ikoma K, Maki M, Ohkawa H, et al. In vivo three-dimensional analysis of hindfoot kinematics. Foot Ankle Int. 2009;30:1094–100.
14. Kido M, Ikoma K, Imai K, Maki M, Takatori R, Tokunaga D, et al. Load response of the tarsal bones in patients with flatfoot deformity: in vivo 3D study. Foot Ankle Int. 2011;32:1017–22.
15. Kimura T, Kubota M, Taguchi T, Suzuki N, Hattori A, Marumo K. Evaluation of first-ray mobility in patients with hallux valgus using weight-bearing CT and a 3-D analysis system: a comparison with normal feet. J Bone Joint Surg Am. 2017;99:247–55.
16. Mosca VS. Flexible flatfoot in children and adolescents. J Child Orthop. 2010;4:107–21.
17. Yamashita T, Yamashita K, Sato M, Kawasumi M, Ata S. Foot-surface-structure analysis using a smartphone-based 3D foot scanner. Med Eng Phys. 2021;95:90–6.
18. Yamashita K, Yamashita T, Sato M, Kawasumi M, Takase Y. Development of a quantitative measurement system for three-dimensional analysis of foot morphology using a smartphone. Annu Int Conf IEEE Eng Med Biol Soc. 2019;2019:3171–4.
19. Volpon JB. Footprint analysis during the growth period. J Pediatr Orthop. 1994;14:83–5.
20. Waseda A, Suda Y, Inokuchi S, Nishiwaki Y, Toyama Y. Standard growth of the foot arch in childhood and adolescence—derived from the measurement results of 10,155 children. Foot Ankle Surg. 2014;20:208–14.
21. Myerson MS. Adult acquired flatfoot deformity: treatment of dysfunction of the posterior tibial tendon. Instr Course Lect. 1997;46:393–405.
22. King DM, Toolan BC. Associated deformities and hypermobility in hallux valgus: an investigation with weightbearing radiographs. Foot Ankle Int. 2004;25:251–5.
23. Mølgaard C, Lundbye-Christensen S, Simonsen O. High prevalence of foot problems in the Danish population: a survey of causes and associations. Foot. 2010;20:7–11.

Publisher's Note